DOI: 10.1002/ejic.200700501

[1,2,5]Selenadiazolo[3,4-*c*][1,2,5]thiadiazole and [1,2,5]Selenadiazolo-[3,4-*c*][1,2,5]thiadiazolidyl – A Synthetic, Structural, and Theoretical Study

Irina Yu. Bagryanskaya,[a] Yuri V. Gatilov,[a] Nina P. Gritsan,*[b,c] Vladimir N. Ikorskii,[d] Irina G. Irtegova,[a] Anton V. Lonchakov,[c] Enno Lork,[e] Ruediger Mews,*[e] Victor I. Ovcharenko,*[d] Nikolay A. Semenov,[f] Nadezhda V. Vasilieva,[a] and Andrey V. Zibarev*[a,c]

Dedicated to Professor Neil Bartlett on the occasion of his 75th birthday

Keywords: Density functional calculations / Magnetic properties / Nitrogen heterocycles / Radical anions / Sulfur / Selenium

A new heterocyclic system, namely [1,2,5]selenadiazolo[3,4-*c*][1,2,5]thiadiazole (**1**), has been prepared in 60 % yield by the 1:1 condensation of 3,4-diamino-1,2,5-thiadiazole (**4**) with $SeCl_4$ in the presence of pyridine. The structures of **1** and its 1:1 complex with pyridinium chloride (**5**) have been elucidated by X-ray diffraction (XRD). The reversible electrochemical reduction of **1**, as well as its chemical reduction with PhS^- anion, provide the long-lived [1,2,5]selenadiazolo[3,4-*c*][1,2,5]thiadiazolidyl radical anion (**2**), which has been isolated in the form of the thermally stable salt [K(18-crown-6)][**2**] (**3**) in 75 % yield. The experimental structural and spectral characteristics of **1** and **2** agree fairly well with those obtained from density functional (DFT) calculations. The salt **3** has been characterized by ESR spectroscopy (in the solid state and in solution) and XRD. The radical anion **2** acts as a bridging ligand in crystalline **3**. Magnetic measurements on salt **3** reveal weak antiferromagnetic interactions ($J = -1.65$ cm^{-1}). The magnetic structures of **3** and its disulfur congener **11** have been analyzed in terms of dimeric exchange integrals calculated by spin-unrestricted broken-symmetry DFT and post-HF methods.

Introduction

Chalcogen-nitrogen chemistry[1] has begun to play an increasingly important role in the design and synthesis of molecular materials, especially conducting, superconducting and magnetic materials, during the past two decades.[2–7] In particular, numerous spin-carrying chalcogen-nitrogen compounds, mostly neutral and positively charged heterocyclic thiazyl radicals (radical cations), have been carefully explored as molecular magnets and/or conductors. Related negatively charged systems (radical anions) have been less studied as they are much rarer.[1–6]

We have recently described the preparation and X-ray diffraction (XRD) and ESR characterization of thermally stable salts of the [1,2,5]thiadiazolo[3,4-*c*][1,2,5]thiadiazolidyl radical anion.[8] This π-delocalized radical anion might be of interest in materials science as a building block for molecular ion-based magnets and/or conductors.[8–10] Indeed, the results of magnetic susceptibility (χ) measurements on its salts in the temperature range 2–300 K have revealed low-temperature antiferromagnetic ordering of their spin systems. Investigation of the electrical properties of the salts is in progress. One of the directions of further development in this field relates to the Se analogue of [1,2,5]-thiadiazolo[3,4-*c*][1,2,5]thiadiazolidyl, namely [1,2,5]selenadiazolo[3,4-*c*][1,2,5]thiadiazolidyl.

[a] Institute of Organic Chemistry, Russian Academy of Sciences, 630090 Novosibirsk, Russia
Fax: +7-383-330-9752
E-mail: zibarev@nioch.nsc.ru
[b] Institute of Chemical Kinetics and Combustion, Russian Academy of Sciences, 630090 Novosibirsk, Russia
Fax: +7-383-330-7350
E-mail: gritsan@kinetics.nsc.ru
[c] Department of Physics, Novosibirsk State University, 630090 Novosibirsk, Russia
[d] International Tomography Center, Russian Academy of Sciences, 630090 Novosibirsk, Russia
Fax: +7-383-333-1399
E-mail: Victor.Ovcharenko@tomo.nsc.ru
[e] Institute for Inorganic and Physical Chemistry, University of Bremen, 28334 Bremen, Germany
Fax: +49-421-218-4267
E-mail: mews@chemie.uni-bremen.de
[f] Department of Natural Sciences, Novosibirsk State University, 630090 Novosibirsk, Russia

Herein we report on the synthesis of [1,2,5]selenadiazolo[3,4-*c*][1,2,5]thiadiazole (**1**) and its electrochemical and chemical reduction to [1,2,5]selenadiazolo[3,4-*c*][1,2,5]thiadiazolidyl (**2**), which is isolated in the form of the thermally stable salt [K(18-crown-6)][**2**] (**3**; Scheme 1). The crystal and molecular structures of **1** and **3** are elucidated by XRD and the radical anion **2** is characterized by ESR spectroscopy in solution. The salt **3** is also characterized by ESR spectroscopy as well as by magnetic susceptibility measurements in the temperature range 2–300 K. The experimental structural and spectral characteristics of **1** and **2** and the magnetic properties of **3** are compared with those calculated by density functional (DFT) and post-Hartree–Fock (HF) techniques.

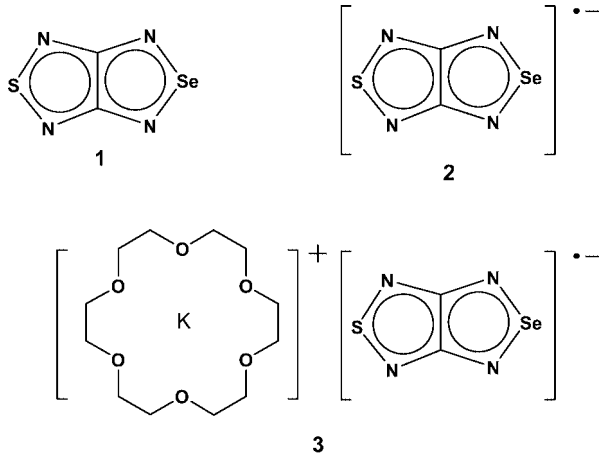

Scheme 1.

It should be noted that beyond the field of chalcogen-nitrogen chemistry, π-delocalized radical anions suitable as spin-carrying units for molecular materials are also very rare and are represented mainly by those derived from nitrogen heterocycles, such as tetrazines,[11] cyanocarbons, such as tetracyanoethylene and 7,7,8,8-tetracyanoquinodimethane,[12] and semiquinones.[13]

Results and Discussion

Preparation and Characterization of [1,2,5]Selenadiazolo[3,4-*c*][1,2,5]thiadiazole (1)

An initial attempt to prepare compound **1** by treating 3,4-diamino-1,2,5-thiadiazole (**4**) with $SeOCl_2$ in the presence of pyridine was unsuccessful. The reaction product was described as an unstable solid with no reported characteristics (even melting point) other than a low-resolution mass spectrum.[14]

In this work, compound **1** is synthesized in 60% yield by the 1:1 condensation of diamine **4** with $SeCl_4$ in the presence of pyridine (Scheme 2). This approach is an extension of the chalcogen tetrahalide based methodology, previously suggested for the synthesis of 2,1,3-benzochalcogenadiazoles, to non-benzoid systems (chalcogen tetrahalides are SF_4, $SeCl_4$, and $TeCl_4$).[15] Unexpectedly, compound **1** was isolated from the reaction mixture in the form of a 1:1 complex with pyridinium chloride (**5**; Scheme 2). Pure **1**, which was obtained by decomposition of complex **5** with water, was found to be thermally stable and stable to air in both the solid state and in solution.

The structures of **1** and **5** were confirmed by XRD (Figures 1 and 2, respectively). The pyridinium cation in the crystal of **5** is disordered over two positions in each of which the N atom is also disordered over two positions (Figure 2). In the crystal of **1**, the molecules lie in the crystallographic *m* plane. Only half a molecule is crystallographically independent since the crystallographic C_2 axis passes through the center of the C–C bond, which means that either S or Se atoms can be placed in the same position. The best refinement was achieved with occupation factors (SOF) of 0.25 for both S and Se (Figure 1). As a result, the experimental accuracy of the molecular geometry of **1** is higher in the case of its co-crystal with pyridinium chloride **5** than in the case of its homo-crystal (see Figures 1 and 2). The experimental geometry of **1** in complex **5** agrees well with its geometry calculated at the DFT/B3LYP/6-31G(d) level of theory (Figure 2).

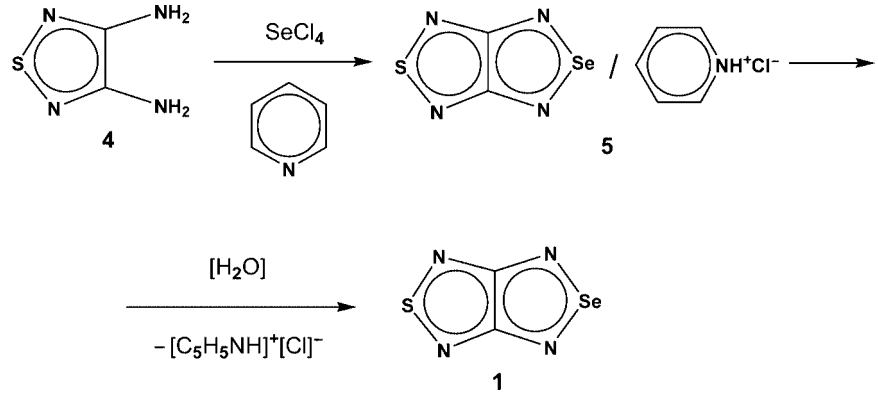

Scheme 2.

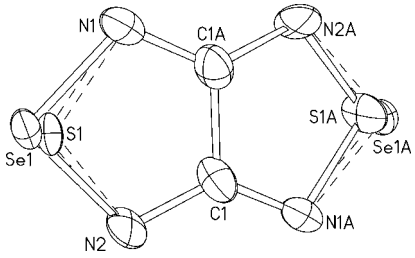

Figure 1. Structure of compound **1**. Bond lengths [pm] and angles [°]: Se1–N1 177.6(9), Se1–N2 182.1(9), S1–N2 158(2), S1–N1 165(2), N2–C1 134.1(8), N1–C1A 130.9(8), C1–C1A 148.9(13); N1–Se1–N2 93.0(4), N2–S1–N1 107.8(9), C1–N2–S1 101.4(8), C1–N2–Se1 107.4(5), C1A–N1–S1 100.7(8), C1A–N1–Se1 109.6(5), N1A–C1–N2 129.7(6), N1A–C1–C1A 115.4(8), N2–C1–C1A 114.6(8) [symmetry transformation used: $-x$, y, $-z + 2$].

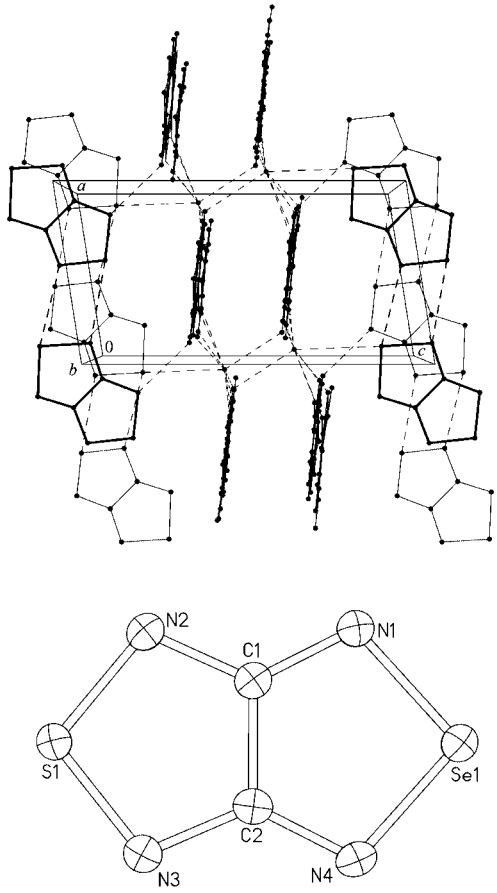

Figure 2. Top: structure of compound **5** (dotted lines show shortened intermolecular contacts). Bottom: compound **1** (XRD numbering is used) moiety in **5**; bond lengths [pm] and angles [°]: Se1–N1 179.0(4), Se1–N4 179.7(4), N1–C1 133.2(6), N4–C2 133.0(6), C1–C2 144.7(6), S1–N2 163.0(5), S1–N3 162.6(4), N2–C1 135.3(6), N3–C2 136.0(6); N1–Se1–N4 95.74(18), Se1–N1–C1 105.0(3), N1–C1–C2 117.3(4), C2–C1–N2 114.2(4), C1–N2–S1 104.9(3), N2–S1–N3 102.5(2), S1–N3–C2 105.2(3), N3–C2–C1 113.3(4), C1–C2–N4 117.0(4), C2–N4–Se1 105.0(3). Bond lengths [pm] and angles [°] of the same moiety obtained from DFT/B3LYP/6-31G(d) calculations: Se1–N1 (Se1–N4) 179.5, N1–C1 (N4–C2) 133.0, C1–C2 147.0, S1–N2 (S1–N3) 163.0, N2–C1 (N3–C2) 135.0; N1–Se1–N4 97.4, Se1–N1–C1 104.1, N1–C1–C2 117.3, C2–C1–N2 113.6, C1–N2–S1 (S1–N3–C2) 104.7, N2–S1–N3 102.9, N3–C2–C1 113.5, C1–C2–N4 116.8, C2–N4–Se1 104.6.

The formation of [1,2,5]selenadiazolo[3,4-*c*][1,2,5]selenadiazole (**6**) as a minor by-product in the preparation of **1** was observed by mass spectrometry and confirmed by XRD characterization in the form of a statistically disordered co-crystal of **1** with **6** ("compound" **7**; Scheme 3, Figure 3). The best refinement was achieved with occupation factors (SOF) in the S2/Se2 position of 0.56 for S and 0.44 for Se (Figure 3). As a result, the experimental accuracy was relatively low, which makes a correct comparison of the changes in molecular geometry on going from the archetypal [1,2,5]thiadiazolo[3,4-*c*][1,2,5]thiadiazole (**8**)[8b] to **1** and **6** impossible.

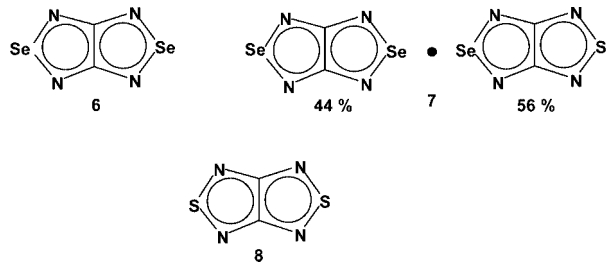

Scheme 3.

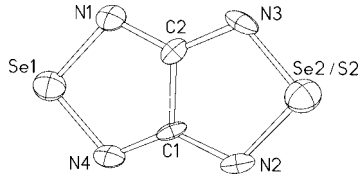

Figure 3. Structure of complex **7** between **1** and **6** (56:44). Bond lengths [pm] and angles [°]: Se1–N1 178(1), Se1–N4 175(1), Se2/S2–N2 169(1), Se2/S2–N23 166(1), N1–C2 132(2), N2–C1 132(2), N3–C2 132(2), N4–C1 131(2), C1–C2 146(2); N1–Se1–N4 94.5(5), N2–Se2/S2–N3 98.0(5), Se1–N1–C2 107.0(9), Se2/S2–N2–C1 107.6(9); Se2/S2–N3–C2 107.0(8), Se1–N4–C1 107.8(8), N4–C1–C2 115.9(12), N1–C2–C1 114.8(11), N2–C1–C2 112.2(11), N3–C2–C1 115.2(12).

A comparison of the spectroscopic properties of **1** and **8** showed the expected similarities. Thus, the maximum absorption wavelength (λ_{max}) of the long-wave band in the electronic absorption spectra (EAS) of **1** and **8** (DME solutions) is found at 353 and 319 nm, respectively. The theoretical EAS of **1** and **8**, calculated at the TD-DFT/B3LYP/6-31+G(d) level of theory, reveal two $\pi \rightarrow \pi^*$ transitions at 359 (f = 0.0430) and 310 nm (f = 0.3203) in the case of **1** and at 331 (f = 0.0522) and 285 nm (f = 0.3361) in the case of **8** (f is the oscillator strength). These theoretical transitions appear as one unresolved band in the experimental EAS of both compounds (Figure 4). In the NMR spectra, the ^{13}C chemical shift of **1** is only 3 ppm downfield from that of **8**.[8b]

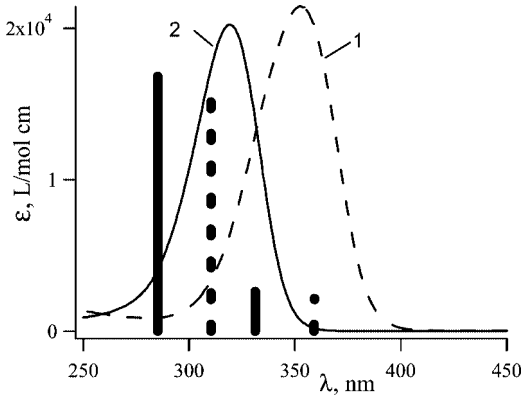

Figure 4. Experimental (curves) EAS of **1** (1) and **8** (2) and theoretical (bars) spectra of **1** (dotted bars) and **8** (solid bars) calculated at the TD-B3LYP/6-31+G(d) level of theory.

Preparation and Characterization of the [1,2,5]Selenadiazolo[3,4-*c*][1,2,5]thiadiazolidyl Radical Anion (2) and the Salt [K(18-crown-6)][2] (3)

Cyclic voltammetry (CV) of a solution of **1** in MeCN in the potential range from 0 to –2.5 V revealed two diffusion-controlled one-electron reduction peaks (1C and 2C, Figure 5) corresponding to consecutive transformations of **1** into the radical anion **2** (peak 1C) and the dianion **9** (peak 2C; Scheme 4). The oxidation peak 1A, which is observed

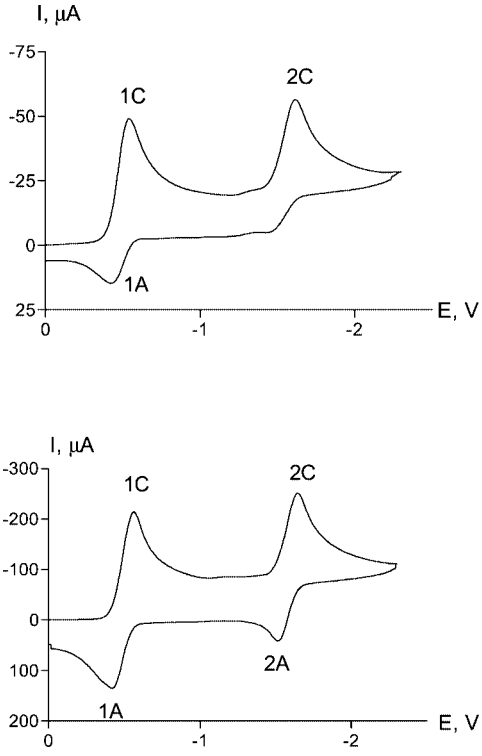

Figure 5. CV of **1** at scan rates of 100 mV s^{-1} (top) and 2 V s^{-1} (bottom).

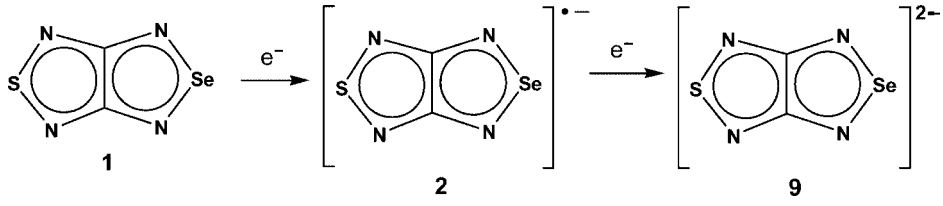

Scheme 4.

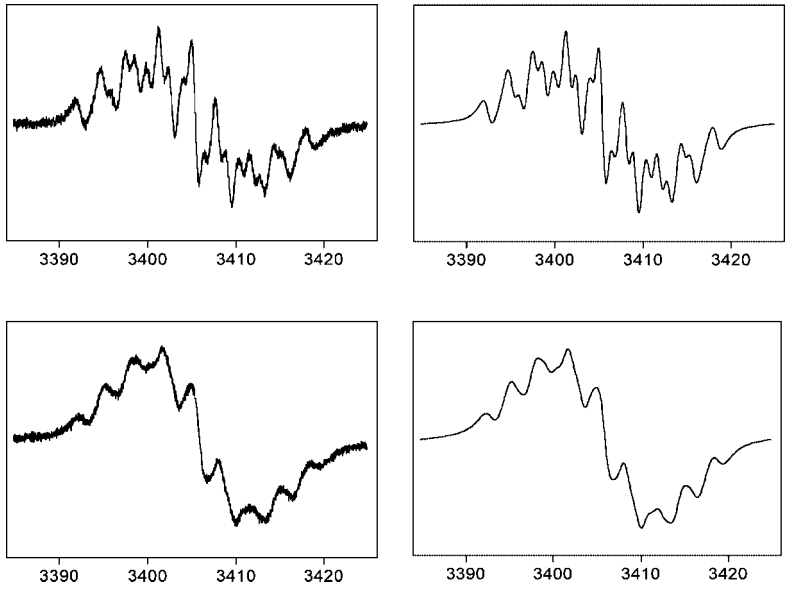

Figure 6. Experimental (in MeCN, left) and simulated (right) ESR spectra of **2** at 223 K (top) and 243 K (bottom). $|H| = 10^{-4}$ T.

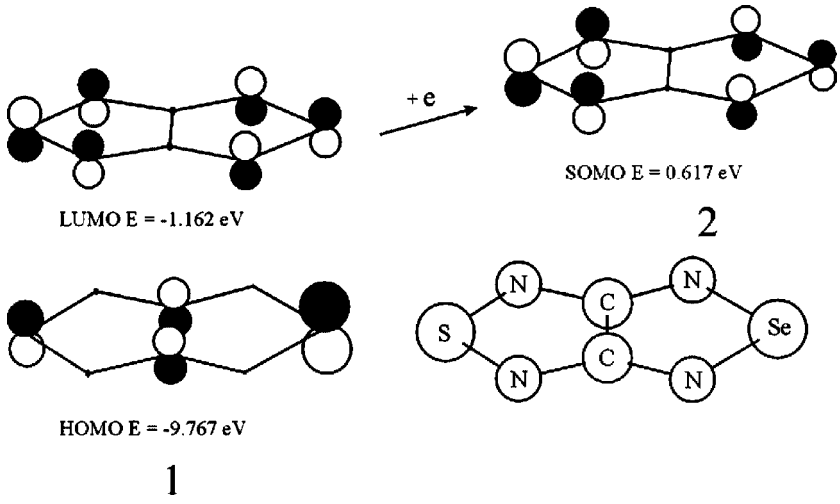

Figure 7. The frontier MOs of **1** and the SOMO of **2** obtained from the HF/6-31G(d) and ROHF/6-31G(d) calculations, respectively, for the molecular geometries optimized at the (U)B3LYP/6-31G(d) level.

even at low scan rates (approx. 10 mV s^{-1}), proves that **2** is a rather long-lived species. The peak potential of reduction 1C in **1** (E_p^{red} = –0.53 V) is only 0.03 V less than the corresponding peak potential of its analog **8**.[8b] Reversibility of the 2C peak of **1** is observed only at scan rates >1 V s^{-1} (Figure 5), which implies that dianion **9** is less stable under the CV conditions than the dianion of **8**.[8b]

The formation of **2** was confirmed by variable-temperature ESR spectroscopy (Figure 6). For **2**, two hfc constants $a(^{14}N \times 2)$ are 0.379 and 0.269 mT, whereas for [1,2,5]thiadiazolo[3,4-*c*][1,2,5] thiadiazolidyl (**10**) $a(^{14}N \times 4)$ is 0.314 mT.[8b] The theoretical hfc constants of **2** calculated at the DFT/UB3LYP/6-31G(d) level of theory [$a(^{14}N_1, ^{14}N_4)$ = 0.360 and $a(^{14}N_2, ^{14}N_3)$ = 0.309 mT] are close to the experimental values.

The ESR spectrum of **2** is temperature-dependent (Figure 6). In the range of 223–295 K it reveals lines broadening with increasing temperature (decreasing solvent viscosity), and at 295 K the spectrum is an unresolved singlet. This behavior is rather uncommon as the inverse situation is normally observed due to better averaging of the anisotropy of both the hfc and the *g*-tensor at higher temperatures. It is not, however, unprecedented, as a similar behavior has been reported for 1,2,3-benzodithiazolyls,[16a] which are neutral thiazyl radicals related to **2**, and explained by spin-rota-

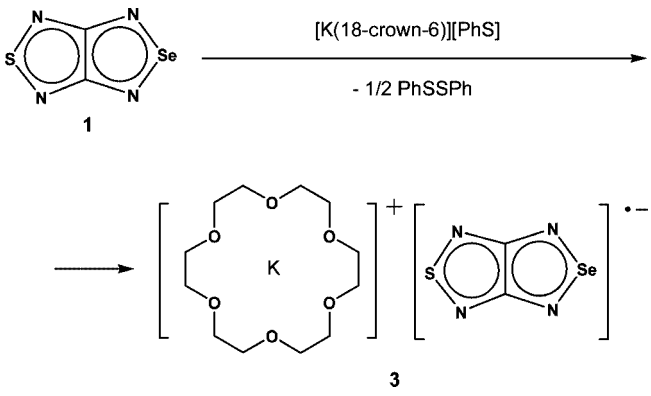

Scheme 5.

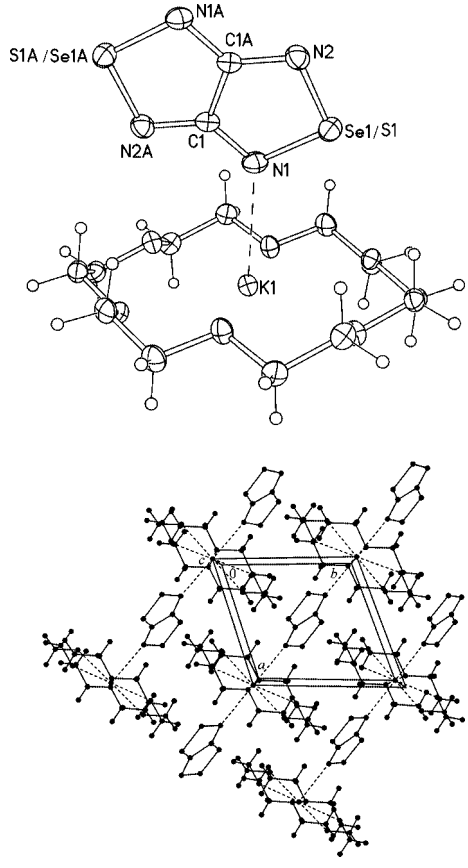

Figure 8. The structure (top) and crystal packing (bottom) of salt **3**. Bond lengths [pm] and bond angles [°] of radical anion **2**: Se1/S1–N1 175.6(4), Se1/S1–N2 174.1(4), N1–C1 133.4(6), N2–C1A 133.8(6), C1–C1A 147.2(8); N1–Se1–N2 97.72(18), Se1–N1–C1 105.3(3), N1–C1–N2A 128.4(4), N1–C1–C1A 115.7(5), N2–C1–C1A115.9(5), C1A–N2–Se1 105.4(3) [symmetry transformation used: –*x* + 1, –*y* + 1, –*z*].

tional relaxation,[16a] which gives an inversely proportional dependence of linewidth on viscosity.[17]

On the basis of the ESR data, the half-life of the electrochemically generated radical anion **2** can be estimated as $\tau_{1/2}$ = 930 s at 243 K and $\tau_{1/2}$ = 750 s at 295 K.

Figure 7 depicts the frontier MOs of **1** and the SOMO of **2** obtained from the HF/6-31G(d) and ROHF/6-31G(d) calculations, respectively, with geometries optimized at the DFT/(U)B3LYP/6-31G(d) level of theory. As usual, the SOMO of **2** is very similar to the LUMO of its neutral precursor **1**.

The thermally stable salt [K(18-crown-6)][**2**] (**3**) was obtained in 75% yield by chemical reduction of **1** with [K(18-crown-6)][PhS] (Scheme 5; see also ref.[8a]).

The structure of salt **3** was confirmed by XRD (Figure 8). As in the case of **1**, either S or Se atoms can be placed in the same position. The best refinement was achieved with occupation factors (SOF) of 0.50 for both S and Se (Figure 8). The crystal packing of **3** is very similar to that of [K(18-crown-6)][**10**][8b] (**11**) and reveals chains along the (01$\bar{1}$) crystallographic direction formed by uniform N···K contacts of 286.7 pm (288.5 pm in salt **11**).[8b] Thus, reduction of the molecular symmetry (disappearance of the inversion center) and the resulting appearance of a dipole moment on going from **10** to **2** essentially does not affect the crystal packing of salts **3** and **11**.

The solid-state ESR spectrum of salt **3**, with an unresolved hyperfine structure and $g_\perp$ = 2.0163 and $g_\parallel$ = 1.9971, is shown in Figure 9. The solution ESR spectrum of **3** in dmf is rather different to the spectrum of the electrochemically generated **2** in MeCN as the spectrum in dmf reveals two hfc constants [$a(^{14}N)$ = 0.380 and $a(^{14}N \times 3)$ = 0.292 mT; Figure 9] with g = 2.001. This difference can be tentatively explained by the reduced molecular symmetry of **2** in the dmf solution of salt **3** (cf., for example, the data for the 2,2′-bipyrimidinyl radical anion in high- and low-symmetry complexes[16b]). The reduced symmetry can be proposed, for example, for a non-dissociated complex [K(18-crown-6)(dmf)][**2**] featuring K^+···**2** coordination similar to that observed in the solid state (Figure 8) and additional coordination of dmf to K^+ (instead of a second molecule of **2** as in the solid state).

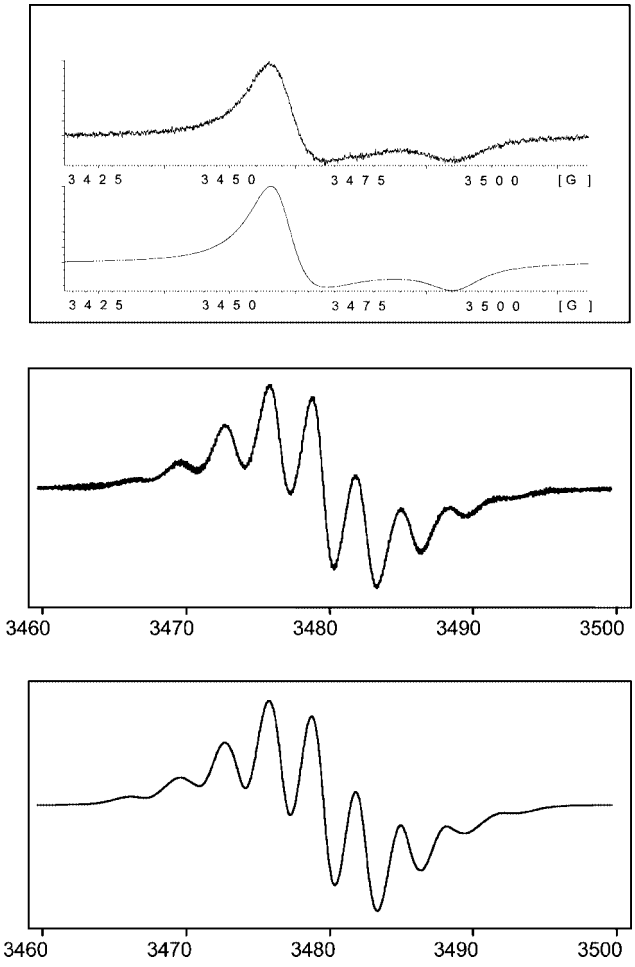

Figure 9. ESR spectra of **3** in the solid state (top: experimental and simulated) and dmf solution (center: experimental; bottom: simulated) at 295 K. $|H|$ 10^{-4} T.

Magnetic Properties of [K(18-crown-6)][2] (3) in Comparison with Those of [K(18-crown-6)][10] (11)

The crystal lattices of salts **3** (this work) and **11**[8a] are very similar; therefore some similarity in their magnetic properties is to be expected. Indeed, the magnetic susceptibility, χ, increases steadily for both salts with a decrease in temperature in the range 300–2 K (Figure 10). The experimental data are best fitted by the Bonner–Fisher uniform chain model[18] with exchange parameters, J, of -1.65 ± 0.03 cm^{-1} (R_2 = 0.997) for **3** and -1.22 ± 0.10 cm^{-1} (R_2 = 0.9997) for **11**.[8a] Thus, within this model, replacement of sulfur by selenium strengthens the antiferromagnetic exchange interactions in the discussed radical anion salts by 35%.

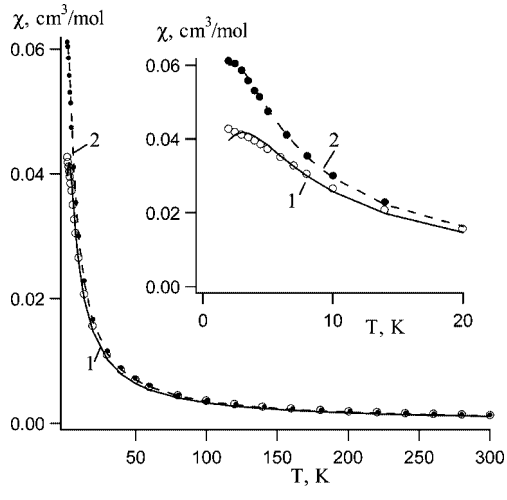

Figure 10. Temperature dependence of χ in the temperature ranges 2–300 K and 2–20 K (inset) for salts **3** (open circles) and **11** (black circles). Theoretical curves: Bonner–Fisher uniform chain model with J = –1.65 cm^{-1} for **3** (1) and J = –1.22 cm^{-1} for **11** (2).

Disordered salt **3** is less suitable for a theoretical analysis of the magnetic properties than salt **11**. Additionally, the symmetry of the radical anion **2** is lower than that of the radical anion **10**, therefore a detailed analysis of the pair exchange interactions (J_{AB}) based on the spin-unrestricted broken-symmetry DFT/UB3LYP/6-31+G(d) calculations was first performed for salt **11**. All radical anions **10** in the crystal of **11** are structurally equivalent. It is therefore possible to select a radical anion and calculate the J_{AB} values with all first-nearest neighbors and then with the closest second-nearest neighbors.

Figure 11 demonstrates that every radical anion **10** has ten first-nearest neighbors, two of which are separated from it by $[K(18\text{-crown-6})]^+$ cations. These ten first-nearest neighbors give only five unique pairs (r1–r5, Figure 11) with the calculated J_{AB} values presented in Table 1. This table also displays the shortest S···S (N···N for r4) distances in the pairs. Only for three of these five pairs are the calculated J_{AB} values higher than the given accuracy of the calculations (0.04 cm^{-1}). All J_{AB} values with closest second-nearest neighbors were found to be less than 0.04 cm^{-1}.

The influence of $[K(18\text{-crown-6})]^+$ cations separating radical anions **10**, as well as that of their 18-crown-6 fragments, on the values of the calculated J_{AB} was estimated in the context of superexchange interactions. J_{AB} was found to be zero for the "bare" r4 pair as well as for r4 pair divided by the $[K(18\text{-crown-6})]^+$ cation (Figure 11). Calculations for the clusters containing pairs r1–r3 and fragments of 18-crown-6 showed a noticeable change of the J_{AB} values

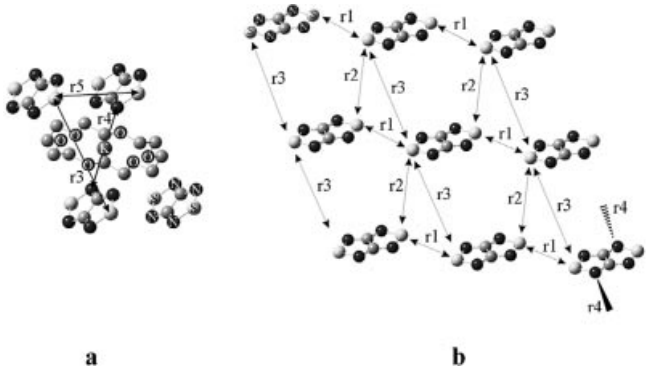

Figure 11. Crystal packing of salt **11** analyzed in terms of shortest intermolecular distances between radical anions **10**: (a) along the $(01\bar{1})$ crystallographic direction (hydrogen atoms of 18-crown-6 are omitted); (b) in the plane perpendicular to this direction.

(Table 1). Figure 12 displays the cluster containing the r3 pair together with two fragments of 18-crown-6 as an example.

Figure 12. Structure of the cluster containing the r3 pair and two fragments of 18-crown-6.

On the whole, the calculations demonstrate that the full magnetic structure of salt **11** is three-dimensional, although J_{AB} for the r1 pair is much larger than all the others (Table 1, Figure 11). The magnetic motif for this salt can therefore be described approximately as a linear spin chain. This is why the $\chi(T)$ dependence is very well fitted by the Bonner–Fisher uniform chain model.[8a] At the same time, the experimentally estimated value of J (-1.22 ± 0.01 cm^{-1}) is about twice as small as J_{AB} calculated for the r1 pair using the spin-unrestricted broken-symmetry approach at the DFT/UB3LYP/6-31+G(d) level of theory.

The HF and post-HF calculations of J_{AB} for the r1 pair, with the same basis set as above, revealed (Table 1) that the UHF and UMP2 calculations considerably underestimate J_{AB}. Note that similar results were recently obtained for model systems such as H···H and H···He···H, where the J_{AB} values were overestimated more than twice with the spin-polarized DFT approach and underestimated by the UHF method; only the UMP4 results agreed well with the data of high-level calculations such as full-CI ones.[19]

As mentioned above, the case of salt **3** is rather complicated since there are three different mutual orientations of the radical anions **2** in the selected pairs (Figure 13). The influence of these orientations on J_{AB} was tested (Table 2). A comparison of Tables 1 and 2 clearly demonstrates that the J_{AB} values for **3** are considerably larger than those for **11**. This observation agrees qualitatively with the difference in the exchange parameter (J) values obtained from the fitting of the $\chi(T)$ dependencies for salts **3** and **11**. At the same time, Table 2 shows that the obtained theoretical mag-

Table 1. Spin-unrestricted broken-symmetry results obtained by the UB3LYP, UHF and UMP2 techniques with the 6-31+G(d) basis set for the dimeric exchange interaction (J_{AB}) of the radical anion **10** with first-nearest neighbors in the crystal of salt **11**.

Pair	Shortest distance in pair [Å]	J_{AB} [cm^{-1}]			
		UB3LYP		UHF	UMP2
		"bare"	with 18-crown-6	"bare"	
r1	S···S, 5.34	2.13	2.79	0.44	0.75
r2	S···S, 6.22	0.09	0.09	–	–
r3	S···S, 8.25	0.26	0.07	–	–
r4	N···N, 5.77	<|0.04|	<|0.04|	–	–
r5	S···S, 8.55	<|0.04|	<|0.04|	–	–

netic motif for salt **3** cannot be correctly described as a uniform spin-chain since three different J_{AB} values alternate along the chain. Indeed, although the experimental $\chi(T)$ dependence for **3** can be fairly well fitted by the Bonner–Fisher uniform chain model, the agreement is not as good as for **11** (see above).

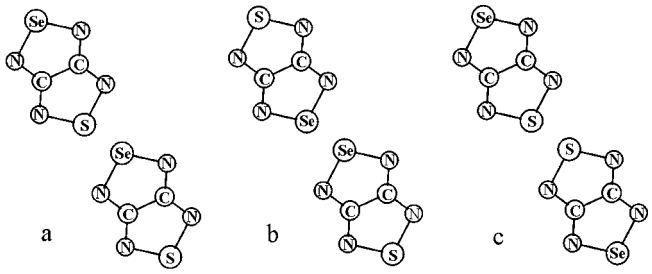

Figure 13. Different mutual orientations of the radical anions **2** reveal the highest J_{AB} values in crystals of salt **3**.

Table 2. Spin-unrestricted broken-symmetry results obtained at the UB3LYP/6-31+G(d) level for the dimeric exchange interaction (J_{AB}) of the radical anion **2** with first-nearest neighbors in the crystal of salt **3** at different mutual orientations (Figure 13).

Pair	J_{AB} [cm^{-1}]		
	a	*b*	*c*
r1	4.02	8.08	1.69
r3	0.37	0.37	0.26

Conclusions

A new heterocyclic system, namely [1,2,5]selenadiazolo[3,4-*c*][1,2,5]thiadiazole (**1**), has been prepared and characterized by XRD. The reversible electrochemical reduction of **1**, as well as its chemical reduction with the PhS$^-$ anion, provide the long-lived [1,2,5]selenadiazolo[3,4-*c*]-[1,2,5]thiadiazolidyl radical anion (**2**), which has been characterized by ESR spectroscopy and isolated in the form of the thermally stable salt [K(18-crown-6)][**2**] (**3**). According to the XRD data, the radical anion **2** acts as a bridging ligand in salt **3**. Magnetic measurements on salt **3** have revealed weak antiferromagnetic interactions (J = –1.65 cm^{-1}). A comparison of **3** with its disulfur congener **11** assuming the Bonner–Fisher uniform chain model has shown that replacement of sulfur by selenium in these radical anion salts enhances the antiferromagnetic exchange interactions by 35%. Theoretical calculations of the exchange interactions in crystals of **3** and **11** have confirmed this trend. At the same time, these calculations demonstrate that the genuine magnetic structures of salts **3** and **11** are three-dimensional. In the case of salt **11**, the exchange interaction (J_{AB}) calculated for one particular type of radical anion pair in the solid state is much larger than for all the others, therefore the theoretical magnetic motif for this salt can be approximately described as a uniform spin chain. The obtained theoretical magnetic motif for salt **3** cannot be correctly described as a uniform spin chain since three different J_{AB} values alternate along the chain.

Experimental Section

General: 3,4-Dichloro-1,2,5-thiadiazole, $SeCl_4$, 18-crown-6, and Ph–S–$SiMe_3$ were used as received from Aldrich, whereas K*t*BuO was sublimed in vacuo before use. 3,4-Diamino-1,2,5-thiadiazole (**4**) was synthesized from the 3,4-dichloro derivative by a known procedure[14] and purified by vacuum sublimation. The complex [K(18-crown-6)][*t*BuO] was prepared as described previously.[20] The syntheses described below were performed under argon in absolutely dry solvents. The ^{1}H and ^{13}C NMR spectra were measured with a Bruker DRX-500 spectrometer at frequencies of 500.13 and 125.76 MHz, respectively, for solutions in $CDCl_3$, with TMS as standard. High-resolution mass spectra (EI, 70 eV) were recorded with a Finnigan MAT MS 8200 mass spectrometer. API-ES mass spectra were recorded with an Agilent 1100 Series LC/MSD instrument. The GC-MS measurements were performed with a Hewlett–Packard G1800A GCD device for solutions in CH_2Cl_2. EAS spectra were recorded with a Hewlett–Packard 8453 instrument for solutions in 1,2-dimethoxyethane (DME). The CV measurements on **1** were performed at 298 K under argon for a 2×10^{-3} M solution of depolarizer in absolute MeCN at a stationary platinum electrode with 0.1 M Et_4NClO_4 as supporting electrolyte, with potential scan rates of 0.01–100 V s^{-1}. Both the 1C and 2C peaks were diffusion-controlled ($I_p^c v^{-1/2}$ = const, where I_p is a current value in the peak and v is a scan rate). Peak potentials are quoted relative to a saturated calomel electrode. The solid-state and solution ESR spectra were recorded with a Bruker ESP-300 spectrometer (MW frequency: 9.7641 GHz; MW power: 265 mW; modulation frequency: 100 kHz; modulation amplitude: 0.005 mT) equipped with a rectangular double resonator and a BST-100/700 temperature control unit. Electrochemical generation of the radical anion **2** from the neutral precursor **1** was performed with a 5×10^{-3} M solution in MeCN (supporting electrolyte: 0.1 M Et_4NClO_4) with a standard cell for variable-temperature ESR measurements under anaerobic conditions. Simulations of the experimental solution ESR spectra were carried out with the Winsim 32 program using the Simplex algorithm of many-parameter optimization for hfc and linewidths. The accuracy in calculating a values is ±0.0001 mT. The solid-state ESR spectrum of salt **3** was simulated with the Simfonia program in the x, y and z directions. Anisotropic hyperfine effects due to the ^{14}N nuclei affect the general linewidth and do not appear directly in the spectrum (Figure 9). The half-life ($\tau_{1/2}$) of the electrochemically generated radical anion **2** in MeCN solution was calculated from the time dependency of the integral intensities of the ESR signals in the absence of an applied potential using the first-order kinetic equation for radical anion decay ($I = Ae^{(-kt)} + B$, $\tau_{1/2} = 0.69\ k^{-1}$). Because of the low solubility of salt **3** in MeCN, its ESR spectrum was recorded in dmf. The g factors of salt **3** in the solid state and dmf solution were measured using a double resonator and MnO standard (six-line spectrum) with an accuracy of ±0.0002. The magnetic measurements were carried out with an MPMS-XL Quantum Design SQUID magnetometer in the temperature range 2–300 K in a magnetic field of 5000 Oe. The molar magnetic susceptibility, χ, of salt **3** was calculated using the standard diamagnetism correction.

Calculations: The quantum chemical calculations were performed with the GAUSSIAN98 program suite.[21] The geometries of the closed-shell compounds and their radical anions were fully opti-

mized at the DFT/(U)B3LYP/6-31G(d) level of theory.[22] The hfc constants were calculated by the same method. The HOMO and LUMO of the closed-shell species and the SOMO of the radical anions were characterized at the HF and ROHF levels of theory, respectively. The EAS were calculated by the TD-DFT/B3LYP/6-31+G(d) technique.[23] For the theoretical analysis of the magnetic structures of **3** and **11**, the exchange integrals (J_{AB}) between selected pairs of radical anions (**2** or **10**, respectively) were calculated using the spin-unrestricted broken-symmetry approach.[24] The J_{AB} values were obtained from the following equation:

$$J_{AB} = E^{S}_{BS} - E^{T}$$

where E^T is the energy of the triplet state of the pair of radical anions and E^S_{BS} is the energy of the open-shell singlet state within the broken-symmetry approach.[24] In all cases the $<S^2>$ value for the broken-symmetry singlet state was about 1.02. The E^T and E^S_{BS} values were calculated using the DFT (UB3LYP), HF (UHF), and post-HF (UMP2) methods with the 6-31+G(d) basis set. The accuracy of the energy calculations was chosen to be 10^{-7} H, which provided values for J_{AB} with an accuracy of 0.04 cm^{-1}.

Crystallographic Analysis: The XRD data (Table 3) for **1**, **3**, **5**, and **7** were collected with a Siemens P4 diffractometer using graphite-monochromated Mo-K_α (λ = 71.073 pm) radiation. The structures were solved by direct methods using the SHELXS-97 program[25] and refined by the least-squares method in the full-matrix anisotropic (isotropic for H atoms) approximation using the SHELXL-97 program.[25] The structures obtained were analyzed for shortened contacts between non-bonded atoms with the PLATON program.[26] CCDC-645192 (for **1**), -644966 (for **3**), -644965 (for **5**), and -645193 (for **7**) contain the supplementary crystallographic data for this paper. These data can be obtained free of charge from The Cambridge Crystallographic Data Centre via www.ccdc.cam.ac.uk/data_request/cif.

Synthesis of Compound 1: A solution of $SeCl_4$ (1.11 g, 0.005 mol) in 15 mL of DME was added dropwise during 10 min to a refluxed and stirred solution of **4** (0.58 g, 0.005 mol) and pyridine (1.58 g, 0.02 mol) in 15 mL of the same solvent. The reaction mixture was refluxed and stirred for an additional 30 min, then filtered hot and cooled to 20 °C. The complex **1**·[C_5H_5NH][Cl] (**5**) was obtained as transparent light-yellow needles (yield: 1.04 g, 68%). M.p. (sealed capillary): 155–157 °C (dec.). $C_7H_6ClN_5SSe$ (306.64): calcd. C 27.42, H 1.97, Cl 11.56, N 22.84; found C 27.27, H 1.82, Cl 11.43, N 22.79. Complex **5** was subsequently treated with H_2O, EtOH, and Et_2O, and the residue was dried under vacuum at 20 °C followed by sublimation at 90 °C/0.1 Torr. According to the API-ES and GC-MS data, the sublimed product was compound **1** (m/z = 191.9 [$C_2N_4S^{80}Se$]) containing approx. 5% of [1,2,5]selenadiazolo[3,4-*c*][1,2,5]selenadiazole (**6**; m/z = 239.8 [$C_2N_4{}^{80}Se_2$]). The

Table 3. Crystal data and structure refinement for compounds **1**, **3**, **5**, and **7**.

Compound	**1**	**3**	**5**	**7**
Empirical formula	C_2N_4SSe	$C_{14}H_{24}KN_4O_6SSe$	$C_7H_6ClN_5SSe$	$C_2N_4S_{0.56}Se_{1.44}$
Formula mass	191.08	494.49	306.64	211.91
Temperature [K]	293(2)[a]	173(2)	173(2)	293(2)
Wavelength [pm]	71.073	71.073	71.073	71.073
Crystal system	monoclinic	triclinic	monoclinic	monoclinic
Space group	*C*2/*m*	$P\bar{1}$	$P2_1/m$	$P2_1/c$
a [pm]	640.4(1)	829.6(2)	639.8(1)	385.0(1)
b [pm]	672.2(2)	852.8(3)	694.2(2)	2208.1(6)
c [pm]	639.4(1)	913.0(2)	1210.6(2)	628.0(2)
α [°]	90	71.08(2)	90	90
β [°]	105.61(1)	63.38(2)	98.93(1)	105.77(3)
γ [°]	90	64.92(2)	90	90
Volume [nm^3]	0.2651(1)	0.5158(2)	0.53117(19)	0.5137(3)
Z	2	1	2	4
Density (calcd.) [$Mg\,m^{-3}$]	2.394	1.592	1.917	2.737
Absorption coefficient [mm^{-1}]	7.351	2.160	3.954	10.552
F(000)	180	253	300	392
Crystal size [mm]	0.31 × 0.30 × 0.03	0.50 × 0.30 × 0.10	0.60 × 0.40 × 0.25	0.20 × 0.20 × 0.07
θ range for data collection [°]	3.31–27.49	2.53–27.49	3.22–27.49	3.50–25.01
Index range	$0 \le h \le 8$ $-8 \le k \le 0$ $-8 \le l \le 8$	$-1 \le h \le 10$ $-10 \le k \le 10$ $-11 \le l \le 11$	$-8 \le h \le 8$ $-9 \le k \le 8$ $-15 \le l \le 15$	$0 \le h \le 4$ $0 \le k \le 26$ $-7 \le l \le 6$
Reflections collected	364	2856	4898	910
Independent reflections	335 [*R*(int) = 0.0313]	2330 [*R*(int) = 0.0302]	1315 [*R*(int) = 0.0334]	774 [*R*(int) = 0.0981]
Completeness to *θ* [%]	100.0	98.3	99.9	84.9
Absorption correction	empirical	empirical	empirical	empirical
Max./min. transmission	0.661/0.204	0.813/0.411	0.382/0.159	0.651/0.179
Refinement method	full-matrix least squares on F^2	full-matrix least squares on F^2	full-matrix least squares on F^2	full-matrix least squares on F^2
Data/restraints/parameters	335/1/32	2330/0/125	1315/12/96	774/0/74
Goodness-of-fit on F^2	1.132	1.033	1.092	1.110
Final *R* indices [$I > 2\sigma(I)$]	R_1 = 0.0461, wR_2 = 0.1270	R_1 = 0.0624, wR_2 = 0.1483	R_1 = 0.0366, wR_2 = 0.0896	R_1 = 0.0743, wR_2 = 0.1851
R indices (all data)	R_1 = 0.0509, wR_2 = 0.1270	R_1 = 0.0932, wR_2 = 0.1649	R_1 = 0.0439, wR_2 = 0.0946	R_1 = 0.1044, wR_2 = 0.2090
Largest difference peak/hole [e Å^3]	0.557/–0.825	0.656/–0.834	0.662/–1.076	0.860/–0.863

[a] The XRD data collected for **1** at 173 K could not be finally refined due to accretion/twinning of the crystal.

product was recrystallized from toluene to give compound **1** as small yellow crystals (yield: 0.57 g, 60%). M.p. (sealed capillary): 231–233 °C. MS: calcd. for $C_2N_4S^{80}Se$ 191.9009; found 191.9028. ^{13}C NMR ($CDCl_3$): δ = 173.6 ppm. EAS (DME): λ_{max} (log ε) = 353 nm (4.33). C_2N_4SSe (191.08): calcd. C 12.57, N 29.32; found C 12.49, N 29.28. The use of Et_3N instead of pyridine led to a mixture of unidentified products. The single crystal of **1** suitable for XRD was obtained by slowly concentrating a DME solution at ambient temperature. The single crystal of **7** (molecular complex between **1** and **6**) was found in the same sample.

Synthesis of Salt 3: A solution of Ph–S–$SiMe_3$ (0.182 g, 0.001 mol) in 2 mL of thf was added to a solution of [K(18-crown-6)][*t*BuO] (0.376 g, 0.001 mol) in 5 mL of the same solvent at –30 °C. The solution was warmed to 20 °C, stirred for 1 h, and the solvent distilled off under vacuum to give a white crystalline residue. Compound **1** (0.191 g; 0.001 mol) and 10 mL of MeCN were then added at –30 °C, and the wine-red solution obtained was warmed to 20 °C, stirred for 1 h, filtered, and the solvents were evaporated under vacuum. The residue was washed with 10 mL of thf, then dissolved in 5 mL of boiling MeCN under normal pressure of argon and the solution cooled to 20 °C. The solvent was removed with a syringe and the crystals that had formed were washed with 10 mL of thf and dried under vacuum. Salt **3** forms transparent ruby plates, Yield: 0.371 g (75%). M.p. (sealed capillary): 138 °C (dec.). $C_{14}H_{24}KN_4O_6SSe$ (494.50): calcd. C 34.00, H 4.89, N 11.33; found C 34.09, H 4.71, N 11.36. Concentration of the initially obtained thf solution gave PhSSPh (98%), as identified by GC-MS techniques by comparison with an authentic sample.

Acknowledgments

The authors are grateful to Prof. Yuri N. Molin and Dr. Leonid A. Shundrin for valuable discussions, to Dr. Alexander Yu. Makarov and Mr. Peter Brackmann for their assistance in the preparative and XRD experiments, respectively, and to the Deutsche Forschungsgemeinschaft (grant 436 RUS 113/486/0-3 R), the Russian Foundation for Basic Research (grants 06-03-32229, 06-03-32742, and 07-03-00467), and the Siberian Division of the Russian Academy of Sciences (interdisciplinary project No. 25) for financial support of this work. N. G. gratefully acknowledges the Ohio Supercomputing Center, USA, for providing computational facilities.

[1] T. Chivers, *A Guide to Chalcogen-Nitrogen Chemistry*, World Scientific, New Jersey, **2005**.

[2] a) K. Awaga, T. Tanaka, T. Shirai, Y. Umezono, W. Fujita, *C. R. Chim.* **2007**, *10*, 52–59; b) K. Awaga, T. Tanaka, T. Shirai, M. Fujimori, Y. Suzuki, H. Yoshikava, W. Fujita, *Bull. Chem. Soc. Jpn.* **2006**, *79*, 25–34; K. Okamoto, T. Tanaka, W. Fujita, K. Awaga, T. Inabe, *Angew. Chem. Int. Ed.* **2006**, *45*, 4516–4518.

[3] a) M. Deumal, S. LeRoux, J. M. Rawson, M. A. Robb, J. J. Novoa, *Polyhedron* **2007**, *26*, 1949–1958; b) J. M. Rawson, A. Alberola, A. Whalley, *J. Mater. Chem.* **2006**, *16*, 2560–2575; c) J. M. Rawson, J. Luzon, F. Palacio, *Coord. Chem. Rev.* **2005**, *249*, 2631–2641; d) J. M. Rawson, F. Palacio, *Struct. Bonding (Berlin)* **2001**, *100*, 93–128; e) J. M. Rawson, G. D. MacManus, *Coord. Chem. Rev.* **1999**, *189*, 135–168; f) J. M. Rawson, A. J. Banister, I. Lavender, *Adv. Heterocycl. Chem.* **1995**, *62*, 137–247.

[4] a) J. L. Brusso, K. Cvrkalj, A. A. Leitch, R. T. Oakley, R. W. Reed, C. M. Robertson, *J. Am. Chem. Soc.* **2006**, *128*, 15080–15081; b) J. L. Brusso, S. Derakhshan, M. E. Itkis, H. Kleinke, R. C. Haddon, R. T. Oakley, R. W. Reed, J. F. Richardson, C. M. Robertson, L. K. Thompson, *Inorg. Chem.* **2006**, *45*, 10958–10966; c) L. Beer, J. L. Brusso, R. C. Haddon, M. E. Itkis, R. T. Oakley, R. W. Reed, J. F. Richardson, R. A. Secco, X. Yu, *Chem. Commun.* **2005**, 5745–5747; d) W. Cordes, R. C. Haddon, R. T. Oakley, *Adv. Mater.* **1994**, *6*, 798–802; e) R. T. Oakley, *Prog. Inorg. Chem.* **1988**, *36*, 299–391.

[5] a) T. S. Cameron, A. Decken, R. M. Kowalczyk, E. J. L. McInnes, J. Passmore, J. M. Rawson, K. V. Shuvaev, L. K. Thompson, *Chem. Commun.* **2006**, 2277–2279; b) A. Decken, S. M. Mattar, J. Passmore, K. V. Shuvaev, L. K. Thompson, *Inorg. Chem.* **2006**, *45*, 3878–3886; c) T. S. Cameron, M. T. Lemaire, J. Passmore, J. M. Rawson, K. V. Shuvaev, L. K. Thompson, *Inorg. Chem.* **2005**, *44*, 2576–2578; d) G. Antorrena, S. Brownridge, T. S. Cameron, F. Palacio, S. Parsons, J. Passmore, L. K. Thompson, F. Zarlaida, *Can. J. Chem.* **2002**, *80*, 1568–1583; e) S. Parsons, J. Passmore, *Acc. Chem. Res.* **1994**, *27*, 101–108.

[6] R. T. Boere, T. L. Roemmele, *Coord. Chem. Rev.* **2000**, *210*, 369–445.

[7] J. Banister, I. B. Gorrell, *Adv. Mater.* **1998**, *10*, 1415–1429.

[8] a) V. N. Ikorskii, I. G. Irtegova, E. Lork, A. Yu. Makarov, R. Mews, V. I. Ovcharenko, A. V. Zibarev, *Eur. J. Inorg. Chem.* **2006**, 3061–3067; b) Yu. Makarov, I. G. Irtegova, N. V. Vasilieva, I. Yu. Bagryanskaya, T. Borrmann, Yu. V. Gatilov, E. Lork, R. Mews, W.-D. Stohrer, A. V. Zibarev, *Inorg. Chem.* **2005**, *44*, 7194–7199.

[9] a) D. Kovisto, R. G. Hicks, *Coord. Chem. Rev.* **2005**, *249*, 2612–2630; b) R. G. Hicks, *Austr. J. Chem.* **2001**, *54*, 597–600.

[10] a) D. Luneau, P. Rey, *Coord. Chem. Rev.* **2005**, *249*, 2591–2611; b) V. I. Ovcharenko, R. Z. Sagdeev, *Russ. Chem. Rev.* **1999**, *68*, 345–365.

[11] a) M. Gloekle, K. Hueber, H.-J. Kuemmerer, G. Denninger, W. Kaim, *Inorg. Chem.* **2001**, *40*, 2263–2269; b) M. Schwach, H.-D. Hausen, W. Kaim, *Inorg. Chem.* **1999**, *38*, 2242–2243.

[12] a) G. Saito, Y. Yoshida, *Bull. Chem. Soc. Jpn.* **2007**, *80*, 1–137; b) K. I. Pokhodnya, M. Bonner, J.-H. Her, P. W. Stephens, J. S. Miller, *J. Am. Chem. Soc.* **2006**, *128*, 15592–15593; c) H. Zhao, R. A. Heintz, X. Ouyang, K. R. Dunbar, C. F. Campana, R. D. Rogers, *Chem. Mater.* **1999**, *11*, 736–746; d) P. J. Kunkeler, P. J. van Koningsbruggen, J. P. Cornelissen, A. N. van der Horst, A. M. van der Kraan, A. L. Spek, J. G. Haasnoot, J. Reedijk, *J. Am. Chem. Soc.* **1996**, *118*, 2190–2197; e) A. Böhm, C. Vazquez, R. S. McLean, J. C. Calabrese, S. E. Kalm, J. L. Manson, A. J. Epstein, J. S. Miller, *Inorg. Chem.* **1996**, *35*, 3083–3088.

[13] a) A. Bencini, C. A. Daul, A. Dei, F. Mariotti, H. Lee, D. A. Shultz, L. Sorace, *Inorg. Chem.* **2001**, *40*, 1582–1590; b) A. Shultz, S. H. Bodnar, K. E. Vostrikova, J. W. Kampf, *Inorg. Chem.* **2000**, *39*, 6091–6093; c) G. Pierpont, C. W. Lange, *Prog. Inorg. Chem.* **1994**, *41*, 331–442; d) M. Adams, A. Dei, A. L. Rheingold, D. N. Hendrickson, *Angew. Chem. Int. Ed. Engl.* **1993**, *32*, 880–882; e) A. Dei, D. Gatteschi, *Inorg. Chim. Acta* **1992**, *198–200*, 813–822.

[14] A. P. Komin, M. Carmack, *J. Heterocycl. Chem.* **1976**, *13*, 13–22.

[15] a) A. V. Zibarev, O. M. Fugaeva, A. O. Miller, S. N. Konchenko, I. K. Korobeinicheva, G. G. Furin, *Khim. Geterotsikl. Soedin.* **1990**, 1124–1133 (in Russian; *Chem. Abstr.* **1991**, *114*, 100927); b) V. Zibarev, A. O. Miller, *J. Fluorine Chem.* **1990**, *50*, 359–563; c) V. N. Kovtonyuk, A. Yu. Makarov, M. M. Shakirov, A. V. Zibarev, *Chem. Commun.* **1996**, 1991–1992; d) F. Cozzolino, J. F. Britten, I. Vargas-Baca, *Cryst. Growth Des.* **2006**, *6*, 181–186.

[16] a) V. Vlasyuk, V. A. Bagryansky, N. P. Gritsan, Yu. N. Molin, A. Yu. Makarov, Yu. V. Gatilov, V. V. Shcherbukhin, A. V. Zibarev, *Phys. Chem. Chem. Phys.* **2001**, *3*, 409–415; b) W. Kaim, *Inorg. Chem.* **1984**, *23*, 3365–3368.

[17] P. W. Atkins, D. Kivelson, *J. Chem. Phys.* **1966**, *44*, 169–174.

[18] W. E. Hatfield, *J. Appl. Phys.* **1981**, *52*, 1985–1990.

[19] T. Soda, Y. Kitagawa, T. Onishi, Y. Takano, Y. Shigeta, H. Nagao, Y. Yoshioka, K. Yamaguchi, *Chem. Phys. Lett.* **2000**, *319*, 223–230.

[20] T. Borrmann, E. Lork, R. Mews, M. M. Shakirov, A. V. Zibarev, *Eur. J. Inorg. Chem.* **2004**, 2452–2458.
[21] M. J. Frisch, G. W. Trucks, H. B. Schlegel, G. E. Scuseria, M. A. Robb, J. R. Cheeseman, V. G. Zakrzewski, J. A. Montgomery Jr, R. E. Stratmann, J. C. Burant, S. Dapprich, J. M. Millam, A. D. Daniels, K. N. Kudin, M. C. Strain, O. Farkas, J. Tomasi, V. Barone, M. Cossi, R. Cammi, B. Mennucci, C. Pomelli, C. Adamo, S. Clifford, J. Ochterski, G. A. Petersson, P. Y. Ayala, Q. Cui, K. Morokuma, D. K. Malick, A. D. Rabuck, K. Raghavachari, J. B. Foresman, J. Cioslowski, J. V. Ortiz, B. B. Stefanov, G. Liu, A. Liashenko, P. Piskorz, I. Komaromi, R. Gomperts, R. L. Martin, D. J. Fox, T. Keith, M. A. Al-Laham, C. Y. Peng, A. Nanayakkara, C. Gonzalez, M. Challacombe, P. M. W. Gill, B. Johnson, W. Chen, M. W. Wong, J. L. Andres, C. Gonzalez, M. Head-Gordon, E. S. Replogle, J. A. Pople, *Gaussian 98 (Revision A.9)*, Gaussian Inc., Pittsburgh, PA, **1998**.
[22] a) P. Geerlings, F. De Proft, W. Langenaeker, *Chem. Rev.* **2003**, *103*, 1793–1873; b) D. Becke, *J. Chem. Phys.* **1993**, *98*, 5648–5652; c) C. Lee, W. Yang, R. G. Parr, *Phys. Rev. B* **1988**, *37*, 785–789.
[23] a) A. Dreuw, M. Head-Gordon, *Chem. Rev.* **2005**, *105*, 4009–4037; b) M. E. Casida, C. Jamorski, K. C. Casida, D. R. Salahub, *J. Chem. Phys.* **1998**, *108*, 4439–4449; c) K. B. Wiberg, R. E. Stratmann, M. J. Frisch, *Chem. Phys. Lett.* **1998**, *297*, 60–64.
[24] a) L. Nudlemann, *J. Chem. Phys.* **1981**, *74*, 5737–5743; b) L. Nudlemann, E. R. Davidson, *Chem. Phys.* **1986**, *109*, 131–143; c) L. Nudlemann, D. A. Case, J. M. Mouesca, *Coord. Chem. Rev.* **1995**, *144*, 199–244; d) H. Nagao, M. Nishino, Y. Shigeta, T. Soda, Y. Kitagawa, T. Onishi, Y. Yoshioka, K. Yamaguchi, *Coord. Chem. Rev.* **2000**, *198*, 265–295; e) M. Deumal, M. J. Bearpark, J. Novoa, M. A. Robb, *J. Phys. Chem. A* **2002**, *106*, 1299–1315.
[25] G. M. Sheldrick, *SHELX-97 – Programs for Crystal Structure Analysis (Release 97-2)*, Institute for Inorganic Chemistry, University of Göttingen, Germany, **1997**.
[26] a) A. L. Spek, *PLATON, A Multipurpose Crystallographic Tool (Version 10 M)*, Utrecht University, The Netherlands, **2003**; b) L. Spek, *J. Appl. Crystallogr.* **2003**, *36*, 7–13.

Received: May 9, 2007
Published Online: September 14, 2007

